Observer-Based Adaptive Sliding Mode Control of NPC Converters: An RBF Neural Network Approach

Yunfei Yin, *Student Member, IEEE*, Jianxing Liu, *Member, IEEE*, Juan Antonio Sánchez, Ligang Wu, *Senior Member, IEEE*, Sergio Vazquez, *Senior Member, IEEE*, José I. Leon, *Fellow, IEEE*, and Leopoldo G. Franquelo, *Fellow, IEEE*

***Abstract*—This paper proposes a novel control strategy for three-level neutral-point-clamped (NPC) power converter. The proposed control scheme consists of three control loops, i.e., instantaneous power tracking control loop, voltage regulation loop, and voltage balancing loop. First, in the power tracking control loop, a set of adaptive sliding mode controllers are established to drive the active and reactive power tracking to their desired values via radial basis function neural network technology. In the voltage regulation loop, an efficient but simple adaptive controller is designed to regulate dc-link output voltage where the load is considered as an external disturbance. Moreover, a composite controller is developed in the voltage balancing loop to ensure imbalance voltages between two dc-link capacitors close to zero, in which a reduced-order observer is used to estimate sinusoidal disturbance improving the converter performance. The effectiveness and superiority of the proposed control strategy for the NPC power converter are compared with other control schemes through experimental results.**

***Index Terms*—Adaptive sliding mode control (SMC), radial basis function neural network (RBFNN), reduced-order observer, three-level neutral-point-clamped (NPC) power converter.**

I. Introduction

NOWADAYS, the problems with environmental pollution and energy crisis cause constant trouble to people. The favorable solution for the above issues is to use the renewable energy sources (RES) such as wind and solar energy, replacing the traditional energy sources. However, high penetration of RES into power systems will result in problems with power stability and quality because of the stochastic characteristic of

Manuscript received January 28, 2018; revised May 10, 2018; accepted June 19, 2018. Date of publication July 3, 2018; date of current version February 20, 2019. This work was supported in part by the National Natural Science Foundation of China under Grants 61525303, 61673130, and 41772377, in part by the Top-Notch Young Talents Program of China (Ligang Wu), in part by the Fundamental Research Funds for the Central Universities under Grant SKLRS201806B, in part by the Andalusian Science and Innovation Project under Grant P11-TIC-7070, and in part by the Spanish Science and Innovation Ministry under Project TEC2016-78430-R. Recommended for publication by Associate Editor Prof. H. Li. (*Corresponding author: Jianxing Liu.)*

Y. Yin, J. Liu, and L. Wu are with the School of Astronautics, Harbin Institute of Technology, Harbin 150001, P. R. China (e-mail:

converter, in which the voltage regulation loop uses PI control and adaptive technique is applied into the instantaneous power tracking loop and voltage balancing loop to resist system parameters uncertainties. An extended state observer (ESO) based second-order sliding mode (SOSM) control scheme has been presented in [34], where PI plus an ESO are used to regulate the sum of capacitor voltages and SOSM controllers are designed to achieve instantaneous active and reactive power tracking and the difference of capacitor voltages balance. Based on the result of [35], the imbalance voltage between the dc-link capacitors is mainly composed of third harmonic component of the grid source voltage. A Luenberger observer designed to estimate the third harmonic voltage component was incorporated into PI controller to allay the influence of the imbalance voltage disturbance in [35]. However, it is observed that most of the reported works still have the following shortcomings.

1) For the voltage regulation loop, the most common solution is the PI controller, which cannot perform well when load changes. In fact, even other advanced controllers like SOSM controller without additional observer still create large overshoot when load changes. However, an additional observer added to the controller make the control structure complex and increase the on-line computation of the processor.
2) For the instantaneous power tracking loop, most of the works cannot consider parametric uncertainties, and the rate of desired instantaneous active and reactive power change are usually neglected or make the assumption knowing its bound.
3) For the voltage balancing loop, individual controller such as PI controller and SOSM controller without additional observer cannot work perfectly, i.e., the imbalance voltage between two capacitors is very big. Several control methods have been presented to deal with this problem. For example, one of the most effective and popular approach is that an observer of asymptotic disturbance rejection, Luenberger observer, is merged into the controller. However, this observer is the full-order observer which is difficult to achieve in practice and increase the on-line computation of processor.

In this paper, a novel control strategy is introduced for the three-phase three-level NPC power converter to overcome the aforementioned problems. In the external loop, an efficient but simple adaptive controller will be designed to regulate dc-link output voltage, where an adaptive law synchronized with controller is designed to adapt the load change. This control method not only overcomes the shortcoming of individual controller but also does not require to add an additional observer. In the internal loop, a set of adaptive sliding mode controllers will be used to drive the active and reactive power tracking their desired values, in which the RBF neural network is utilized to approximate parametric uncertainties and the rate of desired instantaneous active and reactive power change. Compared with the traditional sliding mode control (SMC), the upper bounds of the uncertainties need not be known in advance. In fact, one needs to choose big upper bound in the traditional SMC method to resist the uncertainty; however, this can lead to amplifying the chattering problem. In the voltage balancing loop, a composite

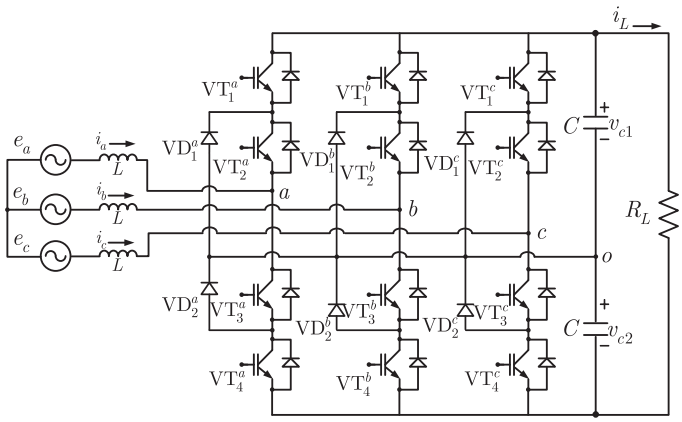

Fig. 1. Three-phase three-level NPC converter.

controller is developed to ensure imbalance voltages between two dc-link capacitors close to zero, in which a reduced-order observer is used to estimate sinusoidal disturbance. Then the reduced-order observer is incorporated into the H_∞ controller whose gain is formulated in terms of linear matrix inequities (LMIs), which can be efficiently solved by MATLAB LMI toolbox. The H_∞ performance index can quantify the disturbance consisting of observation error and other harmonics rejection ability of system.

The remaining part of this paper is organized as follows. In Section II, the state-space averaged model of three-phase three-level grid-connected NPC power converter, basic knowledge of RBFNN, and control objectives are presented. The novel control strategy including instantaneous power tracking loop, voltage regulation loop, and voltage balancing loop for NPC power converter is proposed in Section III. The comparative experimental results between our proposed and other control strategy are presented in Section IV, and conclusions are drawn in Section V.

II. System Description and Preliminaries

A. Converter Description and Modeling

Fig. 1 presents the circuit of a three-phase three-level NPC power converter as a rectifier. At the ac side, the three-phase source voltages e_a, e_b, e_c are connected to the converter through the inductor L. At the dc side, there are two identical capacitors C connected to the load resistance R_L. The converter is composed of three legs with a midpoint connection each, and each leg consists of four insulated-gate bipolar transistors $\mathrm{VT}_i^j, i = \{1,2,3,4\}, j = \{a,b,c\}$, and two clamping diodes $\mathrm{VD}_i^j, i = \{1,2\}, j = \{a,b,c\}$.

Then, the dynamics of inductor currents $i_{\alpha\beta} = [i_\alpha, i_\beta]^{\mathrm{T}}$, the sum of capacitor voltages $x_1 = v_{c1} + v_{c2}$, and the difference of capacitor voltages $x_2 = v_{c1} - v_{c2}$ for the NPC converter can be given in α, β, γ stationary reference frame as [33]

$$\dot{i}_\alpha = \frac{1}{L}v_\alpha - \frac{1}{2L}x_1 u_\alpha + \frac{1}{2\sqrt{6}L}x_2\left(u_\beta^2 - u_\alpha^2\right) - \frac{1}{\sqrt{3}L}x_2 u_\alpha u_\gamma \tag{1}$$

$$\dot{i}_\beta = \frac{1}{L}v_\beta - \frac{1}{2L}x_1 u_\beta + \frac{1}{\sqrt{6}L}x_2 u_\alpha u_\beta - \frac{1}{\sqrt{3}L}x_2 u_\beta u_\gamma \tag{2}$$

$$\dot{x}_1 = -\frac{2}{R_L C}x_1 + \frac{1}{C}i_{\alpha\beta}^{\mathrm{T}}u_{\alpha\beta} \tag{3}$$

$$\dot{x}_2 = \frac{2i_{\alpha\beta}^{\mathrm{T}}u_{\alpha\beta}u_{\gamma}}{\sqrt{3}C} + \frac{1}{\sqrt{6}C}\left[\left(u_{\alpha}^2 - u_{\beta}^2\right)i_{\alpha} - 2u_{\alpha}u_{\beta}i_{\beta}\right] \tag{4}$$

where $v_{\alpha\beta} = [v_\alpha, v_\beta]^{\mathrm{T}}$ is the grid source voltage and $u_{\alpha\beta\gamma} = [u_\alpha, u_\beta, u_\gamma]^{\mathrm{T}}$ is the average duty cycle. Based on the instantaneous theory [36], instantaneous active and reactive powers p, q are defined as

$$\begin{aligned} p &= v_\alpha i_\alpha + v_\beta i_\beta \\ q &= v_\alpha i_\beta - v_\beta i_\alpha. \end{aligned} \tag{5}$$

In order to more conveniently and efficiently design controller, assume that the grid source voltages are balanced and the difference of capacitor voltages x_2 approximates to zero. Then, taking the derivative of (5), one can obtain

$$\begin{aligned} \dot{p} &= -\frac{1}{2L}v_{\alpha\beta}^{\mathrm{T}}u_{\alpha\beta}x_1 + \omega q + \frac{1}{L}\|v_{\alpha\beta}\|^2 \\ \dot{q} &= -\frac{1}{2L}v_{\alpha\beta}^{\mathrm{T}}J^{\mathrm{T}}u_{\alpha\beta}x_1 - \omega p \end{aligned} \tag{6}$$

where $J = \begin{bmatrix} 0 & -1 \\ 1 & 0 \end{bmatrix}$.

The equilibrium point of the system, i.e., $\dot{p} = 0$ and $\dot{q} = 0$ can be obtained from [34]

$$u_{\alpha\beta}^{eq} = \frac{2}{x_1}\left\{\left(1 + \frac{\omega Lq}{\|v_{\alpha\beta}\|^2}\right)v_{\alpha\beta} - \left(\frac{\omega Lp}{\|v_{\alpha\beta}\|^2}\right)Jv_{\alpha\beta}\right\}. \tag{7}$$

B. RBFNN

In this paper, RBFNN will be adopted to approximate the unknown function $d(x)$ in the developed control design procedure for the NPC power converter. For a continuous function $d(x)$ on a compact set $\sqcup$ and ε_m, there exists a RBFNN $\theta^{\mathrm{T}}\xi(x)$ such that

$$\sup_{x\in\sqcup}\left|d(x) - \theta^{\mathrm{T}}\xi(x)\right| \le \varepsilon_m \tag{8}$$

where $\theta = [\theta_1, \theta_2, ..., \theta_l]^{\mathrm{T}}$ is the weight vector, and $\xi(x) = [\xi_1(x), \xi_2(x), ..., \xi_l(x)]^{\mathrm{T}}$ is the basis function vector commonly used Gaussian function

$$\xi_i(x) = \frac{1}{\sqrt{2\pi}\sigma_i}e^{-\frac{1}{2}\left(\frac{\|x-\phi_i\|^2}{\sigma_i}\right)^2},\ i = 1, 2, ..., l \tag{9}$$

where σ_i and ϕ_i are the width and center of the basis function, respectively.

It has been proved that in [37] and [38], the RBFNN can be used to approximate any smooth nonlinear functions $d(t)$ within arbitrary accuracy.

C. Control Objectives

Based on the state-space equation (3), (4), and (6) of the NPC converter, one should design an efficient control scheme to accomplish the following objectives:

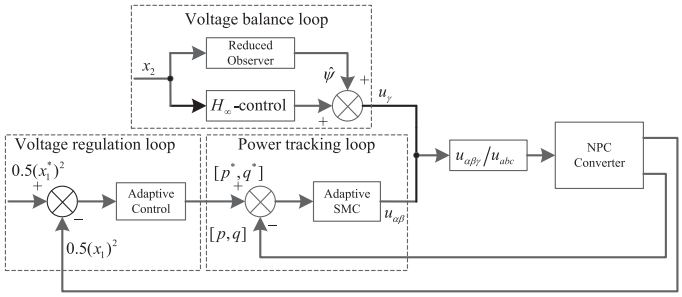

Fig. 2. Flowchart of the proposed control strategy.

1) regulating the sum of capacitor voltages x_1 to its desired value for the supplied load;
2) enforcing instantaneous active and reactive power p, q to track their references, respectively;
3) guaranteeing the imbalance of the capacitor voltages x_2 close to zero.

In the following sections, to control dynamics of the ac/dc NPC power converter, a control method based on DPC strategy is proposed.

III. Controller Design

Based on dynamical model and control objectives of NPC converter, note that it is essential to design three control loops to realize control targets described in the above section. First, a set of adaptive sliding mode controllers are designed in the internal loop to guarantee tracking of instantaneous active and reactive power towards their references. In the second step, an outer loop is established to force the sum of capacitor voltages to a desired constant reference. Finally, a voltage balance loop is built up by H_∞ controller plus reduced-order observer to cope with the imbalance of the capacitor voltages issue. A flowchart of the proposed control strategy is shown in Fig. 2.

A. Instantaneous Power Tracking Loop Design

In this subsection, a set of adaptive sliding mode controllers will be applied to the instantaneous power tracking loop to achieve control objectives via RBF neural network technology. We define the tracking errors as

$$\begin{aligned} e_p &= p^* - p \\ e_q &= q^* - q. \end{aligned} \tag{10}$$

Using (6), time-derivation of (10) yields

$$\begin{aligned} \dot{e}_p &= -\omega q + \frac{v_{\alpha\beta}^{\mathrm{T}}x_1}{2L}u_{\alpha\beta} - \frac{\|v_{\alpha\beta}\|^2}{L} + \dot{p}^* \\ \dot{e}_q &= \omega p + \frac{(Jv_{\alpha\beta})^{\mathrm{T}}x_1}{2L}u_{\alpha\beta} + \dot{q}^*. \end{aligned} \tag{11}$$

Here, note that the above system is an ideal model without considering uncertain parameters. However, in practical applications, the converters are always affected by many factors such as parametric uncertainties, measurement errors, and unknown disturbances, etc. Therefore, it is necessary to establish more accurate model close to the real system behavior. For this rea-

son, the following system where uncertainties are considered in the converter model is represented as

$$\begin{aligned}\dot{e}_p &= -(\omega+\Delta_\omega)q + \left(\frac{1}{2L}+\Delta_L\right)v_{\alpha\beta}^{\mathrm{T}}x_1u_{\alpha\beta} \\ &\quad -\left(\frac{1}{L}+\Delta_L\right)\|v_{\alpha\beta}\|^2+\dot{p}^* \\ \dot{e}_q &= (\omega+\Delta_\omega)p+\left(\frac{1}{2L}+\Delta_L\right)(Jv_{\alpha\beta})^{\mathrm{T}}x_1u_{\alpha\beta}+\dot{q}^* \quad (12)\end{aligned}$$

where Δ_ω and Δ_L are the parametric uncertainties. Then (12) can be rewritten as

$$\begin{aligned}\dot{e}_p &= -\omega q+\frac{v_{\alpha\beta}^{\mathrm{T}}x_1}{2L}u_{\alpha\beta}-\frac{\|v_{\alpha\beta}\|^2}{L}+d_p(t) \\ \dot{e}_q &= \omega p+\frac{(Jv_{\alpha\beta})^{\mathrm{T}}x_1}{2L}u_{\alpha\beta}+d_q(t) \quad (13)\end{aligned}$$

where

$$\begin{aligned}d_p(t) &= -\Delta_\omega q+\Delta_L v_{\alpha\beta}^{\mathrm{T}}x_1u_{\alpha\beta}-\Delta_L\|v_{\alpha\beta}\|^2+\dot{p}^* \\ d_q(t) &= \Delta_\omega p+\Delta_L(Jv_{\alpha\beta})^{\mathrm{T}}+\dot{q}^*. \quad (14)\end{aligned}$$

Next, on the basis of equilibrium point (7), the control signal $u_{\alpha\beta}$ against parametric uncertainties to drive the active and reactive power tracking their desired values are designed as

$$u_{\alpha\beta}=u_{\alpha\beta}^{eq}-\mu(e_p)v_{\alpha\beta}-\mu(e_q)Jv_{\alpha\beta} \quad (15)$$

where $\mu(e_p)$ and $\mu(e_q)$ are the adaptive sliding mode controllers to be designed. Substituting (15) into (13), one can obtain that

$$\begin{aligned}\dot{e}_p &= -\frac{x_1}{2L}\|v_{\alpha\beta}\|^2\mu(e_p)+d_p(t) \\ \dot{e}_q &= -\frac{x_1}{2L}\|v_{\alpha\beta}\|^2\mu(e_q)+d_q(t). \quad (16)\end{aligned}$$

Utilizing the RBFNN to approximate the unknown function $d_p(t)$ and $d_q(t)$, the approximate expressions are

$$\begin{aligned}d_p(t) &= \theta_p^{*\mathrm{T}}\xi+\varepsilon_p,\ \ |\varepsilon_p|\le\varepsilon_{mp} \\ d_q(t) &= \theta_q^{*\mathrm{T}}\xi+\varepsilon_q,\ \ |\varepsilon_q|\le\varepsilon_{mq} \quad (17)\end{aligned}$$

where $\theta_p^{*\mathrm{T}}$ and $\theta_q^{*\mathrm{T}}$ are the ideal weight vector, ε_p and ε_q are the approximation errors, and ε_{mp} and ε_{mq} are their upper bounds, respectively.

A set of adaptive sliding mode controllers by using RBFNN to approximate unknown functions are designed as

$$\begin{aligned}\mu(e_p) &= k_pe_p+\frac{2L}{x_1\|v_{\alpha\beta}\|^2}\left[\hat{\theta}_p^{\mathrm{T}}\xi+\varepsilon_{mp}\mathrm{sign}(e_p)\right] \\ \mu(e_q) &= k_qe_q+\frac{2L}{x_1\|v_{\alpha\beta}\|^2}\left[\hat{\theta}_q^{\mathrm{T}}\xi+\varepsilon_{mq}\mathrm{sign}(e_q)\right] \quad (18)\end{aligned}$$

where k_p and k_q are the positive constants, and $\hat{\theta}_p$ and $\hat{\theta}_q$ are the estimation of ideal weight vectors θ_p^* and θ_q^*, respectively.

Applying adaptive sliding mode controllers (18) into (16), error dynamic becomes

$$\begin{aligned}\dot{e}_p &= -\frac{x_1}{2L}\|v_{\alpha\beta}\|^2k_pe_p-\hat{\theta}_p^{\mathrm{T}}\xi-\varepsilon_{mq}\mathrm{sign}(e_p)+d_p(t) \\ \dot{e}_q &= -\frac{x_1}{2L}\|v_{\alpha\beta}\|^2k_qe_q-\hat{\theta}_q^{\mathrm{T}}\xi-\varepsilon_{mq}\mathrm{sign}(e_q)+d_q(t). \quad (19)\end{aligned}$$

Construct the following Lyapunov function for the system (19)

$$V_{pq}=\frac{1}{2}e_p^2+\frac{1}{2}e_q^2+\frac{1}{2\gamma_p}\tilde{\theta}_p^{\mathrm{T}}\tilde{\theta}_p+\frac{1}{2\gamma_q}\tilde{\theta}_q^{\mathrm{T}}\tilde{\theta}_q \quad (20)$$

where $\tilde{\theta}_p=\hat{\theta}_p-\theta_p^*$ and $\tilde{\theta}_q=\hat{\theta}_q-\theta_q^*$. Then, one can get the derivative of Lyapunov function V_{pq}

$$\dot{V}_{pq}=e_p\dot{e}_p+e_q\dot{e}_q+\frac{1}{\gamma_p}\tilde{\theta}_p^{\mathrm{T}}\dot{\tilde{\theta}}_p+\frac{1}{\gamma_q}\tilde{\theta}_q^{\mathrm{T}}\dot{\tilde{\theta}}_q. \quad (21)$$

Using (17) and (19), one can get

$$\begin{aligned}\dot{V}_{pq} = &-\frac{x_1}{2L}\|v_{\alpha\beta}\|^2k_pe_p^2-e_p\hat{\theta}_p^{\mathrm{T}}\xi-\varepsilon_{mp}|e_p|+e_p\theta_p^{*\mathrm{T}}\xi \\ &-\frac{x_1}{2L}\|v_{\alpha\beta}\|^2k_qe_q^2-e_q\hat{\theta}_q^{\mathrm{T}}\xi-\varepsilon_{mq}|e_q|+e_q\theta_q^{*\mathrm{T}}\xi \\ &+\frac{1}{\gamma_p}\tilde{\theta}_p^{\mathrm{T}}\dot{\tilde{\theta}}_p+\frac{1}{\gamma_q}\tilde{\theta}_q^{\mathrm{T}}\dot{\tilde{\theta}}_q+\varepsilon_pe_p+\varepsilon_qe_q \\ \le &-\frac{x_1}{2L}\|v_{\alpha\beta}\|^2k_pe_p^2-\frac{x_1}{2L}\|v_{\alpha\beta}\|^2k_qe_q^2-e_p\tilde{\theta}_p^{\mathrm{T}}\xi \\ &-e_q\tilde{\theta}_q^{\mathrm{T}}\xi-(\varepsilon_{mp}-\varepsilon_p)|e_p|-(\varepsilon_{mq}-\varepsilon_q)|e_q|+\frac{1}{\gamma_p}\tilde{\theta}_p^{\mathrm{T}}\dot{\tilde{\theta}}_p \\ &+\frac{1}{\gamma_q}\tilde{\theta}_q^{\mathrm{T}}\dot{\tilde{\theta}}_q. \quad (22)\end{aligned}$$

We design the adaptive law as

$$\begin{aligned}\dot{\tilde{\theta}}_p &= \gamma_pe_p\xi \\ \dot{\tilde{\theta}}_q &= \gamma_qe_q\xi. \quad (23)\end{aligned}$$

Then, using (23), the derivative of Lyapunov function becomes

$$\begin{aligned}\dot{V}_{pq} \le &-\frac{x_1}{2L}\|v_{\alpha\beta}\|^2k_pe_p^2-\frac{x_1}{2L}\|v_{\alpha\beta}\|^2k_qe_q^2 \\ &-(\varepsilon_{mp}-\varepsilon_p)|e_p|-(\varepsilon_{mq}-\varepsilon_q)|e_q|. \quad (24)\end{aligned}$$

Therefore, according to the Lasalle's theorem [39], we can conclude that the track errors $e_p(t)$ and $e_q(t)$ converge to 0 as $t\to\infty$, i.e., the adaptive sliding mode controllers can enforce instantaneous active and reactive power p, q to track their references, respectively. The control structure of instantaneous power tracking loop is shown in Fig. 3.

B. Voltage Regulation Loop Design

In this subsection, an adaptive controller will be designed in the external loop to regulate the sum of capacitor voltages x_1 to its desired value x_1^*. Assume that the equivalent load resistance R_L considered as unknown disturbance is slowing time varying, i.e., $\dot{R}_L\cong 0$, and the dynamics of the instantaneous power are much faster than voltage dynamic. Then, the dynamic of sum of

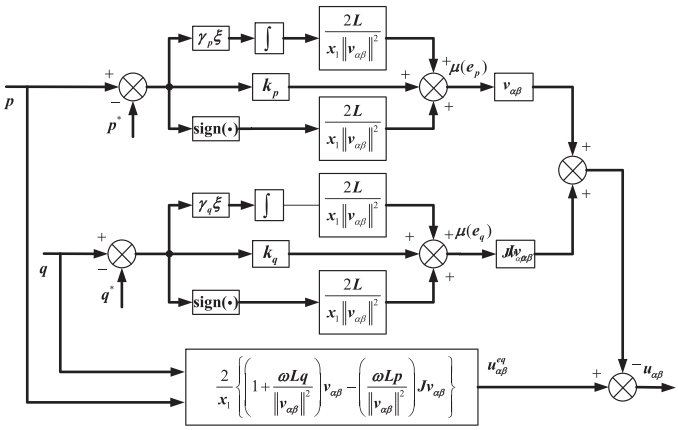

Fig. 3. Adaptive sliding mode controller structure based on the RBF neural network technology.

capacitor voltages x_1 can be rewritten as

$$\dot{x}_1 = -\frac{2}{R_L C}x_1 + \frac{1}{C}i_{\alpha\beta}^{*\mathrm{T}}u_{\alpha\beta} \tag{25}$$

where $i_{\alpha\beta}^*$ is the reference of inductor current $i_{\alpha\beta}$. Then, we have

$$\dot{z}_1 = -\eta z_1 + \frac{2}{C}p^* \tag{26}$$

where $z_1 = \frac{1}{2}x_1^2$ is the new state variable, $p^* = \frac{x_1}{2}i_{\alpha\beta}^{*\mathrm{T}}u_{\alpha\beta}$ is the desired reference of the instantaneous active p and $\eta = \frac{4}{R_L C}$ is the unknown parameter. We define the regulation error as follows:

$$e_z = z_1 - z_1^* \tag{27}$$

where $z_1^* = \frac{x_1^{*2}}{2}$. Following from (26), time-derivation of (27) is

$$\dot{e}_z = \dot{z}_1 = -\eta z_1 + \frac{2}{C}p^*. \tag{28}$$

Next, an efficient but simple adaptive controller will be designed to regulate the sum of capacitor voltages x_1 to its desired value x_1^* as well as provide the power reference for the internal loop.

The following Lyapunov function is constructed to design the adaptive controller

$$V_1(t) = \frac{1}{2}e_z^2 + \frac{1}{2\lambda}\tilde{\eta}^2 \tag{29}$$

where λ is the positive constant, $\tilde{\eta} = \hat{\eta} - \eta$, and $\hat{\eta}$ is the adaptive law to be designed.

Take the derivative of (29) along the system (28)

$$\dot{V}_1 = e_z\left(-\eta z_1 + \frac{2}{C}p^*\right) + \frac{1}{\lambda}\tilde{\eta}\dot{\tilde{\eta}}. \tag{30}$$

We design the following adaptive controller and the adaptive law

$$p^* = -k_{vs}e_z + \frac{C}{2}z_1\hat{\eta} \tag{31}$$

$$\dot{\hat{\eta}}(t) = -\lambda z_1 e_z. \tag{32}$$

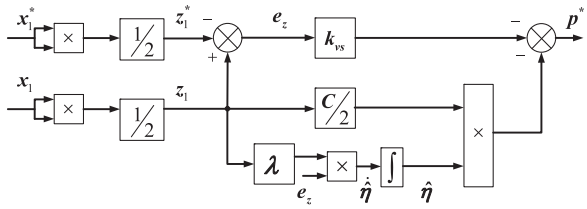

Fig. 4. Adaptive controller in the voltage regulation loop.

Substituting (31) and (32) into (30), yields

$$\begin{aligned}\dot{V}_1 &= -\eta z_1 e_z - \frac{2}{C}k_{vs}e_z^2 + \hat{\eta}z_1 e_z - \tilde{\eta}(t)z_1 e_z \\ &= -\frac{2}{C}k_{vs}e_z^2.\end{aligned} \tag{33}$$

Therefore, according to the Lasalle's theorem [39], we can conclude that the regulation error $e_z(t)$ converge to 0 as $t \to \infty$, that is, an adaptive controller can regulate the sum of capacitor voltages x_1 to its desired value x_1^*. The control structure of voltage regulation loop is shown in Fig. 4.

C. Voltage Balancing Loop Design

In this subsection, a composite controller which consists of H_∞ controller and reduced-order observer will be designed in the balancing loop to ensure imbalance voltages between two dc-link capacitors close to zero. Based on the assumption in the voltage regulation loop, that is, the dynamics of the instantaneous power are much faster than voltage dynamic, one can introduce the equilibrium point (7) of the system into (4). Then, the dynamic of (4) becomes

$$\dot{x}_2 = \frac{4p^*}{C\sqrt{3}x_1}u_\gamma + \frac{1}{C}\psi(t) \tag{34}$$

where $\psi(t)$ is considered as the disturbance in this paper. According to [35], the disturbance $\psi(t)$ mainly consists of a sinusoidal disturbance whose frequency is three times of the fundamental frequency, and can be defined as

$$\psi(t) = \chi \sin(3\omega t + \varphi) \tag{35}$$

where χ and φ are the constant values. Next, a reduced-order observer will be designed to estimate sinusoidal disturbance improving the converter performance.

Adding two new state variables disturbance $\psi(t)$ and its time derivative x_ψ, the augmented system can be expressed as

$$\begin{aligned}\dot{x}_2 &= \frac{h}{C}u_\gamma + \frac{1}{C}\psi \\ \dot{\psi} &= x_\psi \\ \dot{x}_\psi &= -9\omega^2\psi\end{aligned} \tag{36}$$

where $h = \frac{4p^*}{\sqrt{3}x_1}$.

Furthermore, one can obtain the following state space representation

$$\begin{aligned}\dot{x} &= Ax + Bu_\gamma \\ y &= Ex\end{aligned} \tag{37}$$

where $x = [x_2, \psi, x_\psi]^{\mathrm{T}}$ and y stand for system states and measurable output, respectively, and

$$A = \begin{bmatrix} 0 & \frac{1}{C} & 0 \\ 0 & 0 & 1 \\ 0 & -9\omega^2 & 0 \end{bmatrix}, B = \begin{bmatrix} \frac{h}{C} \\ 0 \\ 0 \end{bmatrix}, E = \begin{bmatrix} 1 \\ 0 \\ 0 \end{bmatrix}^{\mathrm{T}}$$

are constant matrices.

Then the system (37) can be rewritten as

$$\begin{bmatrix} \dot{\bar{x}}_1 \\ \dot{\bar{x}}_2 \end{bmatrix} = \begin{bmatrix} A_{11} & A_{12} \\ A_{21} & A_{22} \end{bmatrix} \begin{bmatrix} \bar{x}_1 \\ \bar{x}_2 \end{bmatrix} + \begin{bmatrix} B_1 \\ B_2 \end{bmatrix} u_\gamma$$
$$y = \bar{x}_1 \tag{38}$$

where

$$A_{11} = [0], A_{12} = \begin{bmatrix} \frac{1}{C} & 0 \end{bmatrix}$$
$$A_{21} = \begin{bmatrix} 0 \\ 0 \end{bmatrix}, A_{22} = \begin{bmatrix} 0 & 1 \\ -9\omega^2 & 0 \end{bmatrix}.$$

It can be observed from (38) that $\bar{x}_1$ can be obtained directly from the measurable output y, and we only suffice to estimate the state variable $\bar{x}_2$. In fact, $\bar{x}_1 = x_2$ is the difference of capacitor voltages that can directly measure and $\bar{x}_2 = [\psi,\ x_\psi]^{\mathrm{T}}$ are the disturbance and its time derivative that are impossible to measure directly and need to be estimated. Thus, the following reduced-order state observer is designed to estimate $\bar{x}_2$

$$\dot{\varepsilon} = F\varepsilon + Gy + Hu_\gamma$$
$$\hat{\bar{x}}_2 = M\varepsilon + Ny \tag{39}$$

where F, G, M, and N are the observer gains to be designed.

Denote observation error $e_\psi = \bar{x}_2 - \hat{\bar{x}}_2$, then its dynamic equation can be expressed as

$$\dot{e}_\psi = (A_{22} + LA_{12})e_\psi. \tag{40}$$

Obviously, the observation error $e_\psi \to 0$ if only if $A_{22} + LA_{12}$ is Hurwitz. Based on the result of [40], one can obtain that if there exist positive matrix P such that

$$(A_{22} + LA_{12})^{\mathrm{T}} P + P(A_{22} + LA_{12}) \le 0 \tag{41}$$

then $A_{22} + LA_{12}$ is Hurwitz. The equation (41) is equivalent to

$$A_{22}^{\mathrm{T}} P + PA_{22} + WA_{12} + A_{12}^{\mathrm{T}} W^{\mathrm{T}} \le 0 \tag{42}$$

where $W = PL$.

One can note that the equation (42) is the standard linear matrix inequality, which can be efficiently solved by MATLAB LMI toolbox to obtain the matrices P and Q. Furthermore, the matrix is determined by $L = P^{-1}Q$.

Defining $\varepsilon = \hat{\bar{x}}_2 + Ly$ yields

$$\begin{aligned} \dot{\varepsilon} &= \dot{\hat{\bar{x}}}_2 + L\dot{y} \\ &= (A_{22} + LA_{12})\hat{\bar{x}}_2 + L(A_{11}y + B_1u_\gamma) \\ &\quad + A_{21}y + B_2u_\gamma + (B_2 + LB_1)u_\gamma. \end{aligned} \tag{43}$$

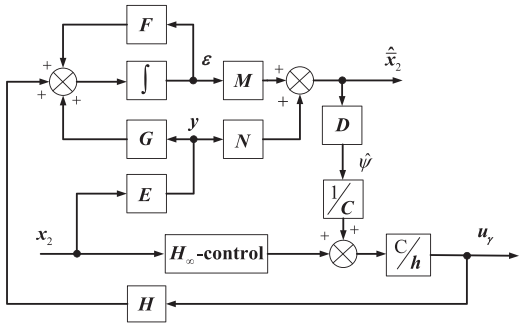

Fig. 5. H_∞ controller structure based on the reduced-order observer.

Fig. 6. Laboratory prototype of three-phase three-level NPC power converter.

TABLE I
PARAMETERS USED FOR SIMULATION

Description	Parameter	Value	Unites
Switching Rate	f_c	$11.2 \cdot 10^3$	Hz
Grid line voltage	e_{abc}	400	V
Phase inductor	L	1.2	mH
dc-link capacitor	C	1100	uF
Load resistance	R_L	$120 \to 60$	Ω
Reference output voltage	x_1^*	750	V

Then one can obtain the observer gains as

$$\begin{aligned} F &= A_{22} + LA_{12} \\ G &= (A_{21} + LA_{11}) - (A_{22} + LA_{12})L \\ H &= B_2 + LB_1 \\ M &= I \\ N &= -L. \end{aligned} \tag{44}$$

Using the estimated disturbance $\psi(t)$, the following composite controller will be designed via H_∞ technique

$$u_\gamma = \frac{C}{h}\left(k_b x_2 + \frac{1}{C}\hat{\psi}\right) \tag{45}$$

where k_b is the H_∞ controller gain to be designed.

Substituting (45) into (34), yields

$$\dot{x}_2 = -k_b x_2 + \frac{1}{C}\varsigma(t) \tag{46}$$

where $\varsigma(t)$ consisting of observation error and other harmonics is the disturbance. Based on the result of [41], the following condition is presented to calculate the admissible H_∞ controller.

TABLE II
CONTROLLERS PARAMETERS

Control strategy	Power tracking loop	Voltage regulation loop	Voltage balancing loop
The proposed control strategy	$k_p = k_q = 1.6 * 10^{-7}$, $\gamma_p = \gamma_q = 8.0 * 10^{-4}$ $\varepsilon_{mp} = \varepsilon_{mq} = 5.0 * 10^{-5}$	$k_{vs} = 0.15$ $\lambda = 2.0 * 10^{-7}$	$L = [-0.8701, -1.79 * 10^3]^{\mathrm{T}}$ $k_b = 1.08 * 10^3$, $\varrho = 4.5$
PI control strategy	$k_{pp} = k_{pq} = 3.54 * 10^{-5}$ $k_{ip} = k_{iq} = 3.54 * 10^{-2}$	$k_{vs} = 0.12$ $k_{iv} = 5$	$k_{pb} = 0.15$ $k_{ib} = 3$

For given constant ϱ, if there exist positive scalars w_b and j_b, such that

$$\begin{bmatrix} 2w_b + 1 & \frac{1}{C} j_b \\ \frac{1}{C} j_b & -\varrho^2 \end{bmatrix} \leq 0 \tag{47}$$

then the system satisfies

1) the difference of capacitor voltages $x_2 = v_{c1} - v_{c2}$ converges to zero as $t \to \infty$ in the absence of disturbance;
2) under zero-initial condition, the following inequality

$$\int_0^{+\infty} x_2^{\mathrm{T}} x_2 dt \leq \varrho^2 \int_0^{+\infty} \varsigma^{\mathrm{T}} \varsigma dt \tag{48}$$

holds in the presence of disturbance input $\varsigma(t)$.

Moreover, if the couple of scalars w_b and j_b are found, we can get H_∞ controller gain as $k_b = \frac{w_b}{j_b}$. The control structure of voltages balancing loop is shown in Fig. 5, where $D = [1, 0]$.

D. Discussion

Three control loops, the instantaneous power tracking control loop, voltage regulation loop, and voltage balancing loop, for three-level NPC power converter are designed to realize control targets in this section. In the instantaneous power tracking control loop, a set of adaptive sliding mode controllers are used to force the active and reactive power tracking to their desired values, in which the RBF neural network is utilized to approximate the unknown disturbance. In comparison with the traditional SMC, adaptive SMC can soften the chattering problem, yet increase the on-line computation of the processor. It is well known that if one wants to accurately estimate the unknown disturbance, the more Gaussian nodes should be chosen. However, the more number of Gaussian nodes one chooses, the more on-line computation the processor takes. In the voltage regulation loop, an efficient but simple adaptive controller is designed to regulate dc-link output voltage. This control method is more effective in suppression of the overshoot without adding an additional observer or feedforward compensation when load change. However, this control approach needs to assume that the equivalent load resistance, as the unknown disturbance, is slowing time varying (possible constant or change in steps). In the voltage balancing loop, an H_∞ controller coupled with reduced observer is adopted to drive imbalance voltages convergence to zero. Compared with full-order observer method, obviously, this method can reduce the on-line computation of the processor. However, in comparison with individual controllers such as PI controller and SOSM controller, this control method improves the system performance at the expense of increasing complexity of computation and control structure. On the other hand, only when the power converter operates at the balanced grid-voltage conditions does the proposed control strategy work perfectly.

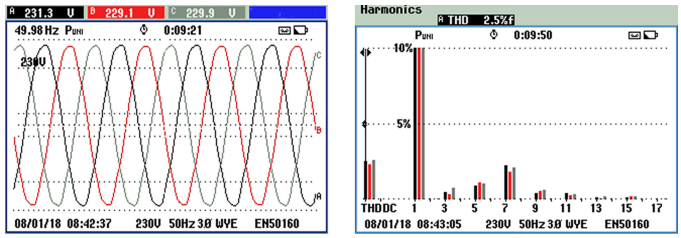

(a) (b)

Fig. 7. Grid voltage. (a) Three-phase voltage. (b) THD of v_a.

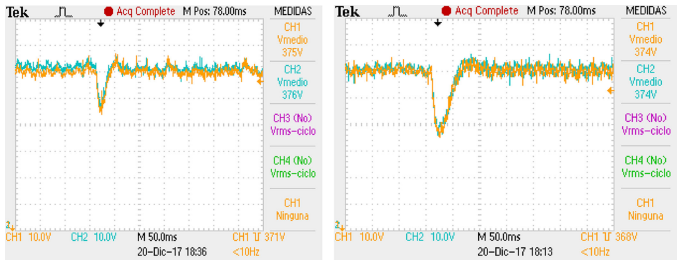

Fig. 8. Responses of capacitor voltages v_{c1} and v_{c2}. (a) Proposed control. (b) PI control.

IV. EXPERIMENTAL RESULTS

In order to verify the effectiveness and superiority of our proposed control strategy, the experimental comparisons using a prototype between our proposed and well tuned PI control strategy are provided in this section. Additional simulation results comparing the proposed strategy with the control in [34] showed similar results. Therefore, only the practical results are included in the paper.

A basic prototype of a three-phase three-level NPC power converter is shown in the Fig. 6 whose parameters are summarized in Table I and the TMS320VC33 floating point digital signal processor board is selected to execute the control algorithm. In this experiment, the grid voltage is distorted and unbalanced to some extend, as it is shown in Fig. 7. Taking into account that the controlled design assumes balanced grid voltage, this situation allows us to test the robustness of the proposed controller under a more realistic environment. The resistance R_L is stepped from no load to the half load (4.6875 kW) then to full load (9.375 kW) and the reactive power is set to 0 VAr. The parameters of our proposed and PI control strategy have been shown in Table II, respectively. Fig. 8(a) and (b) show the

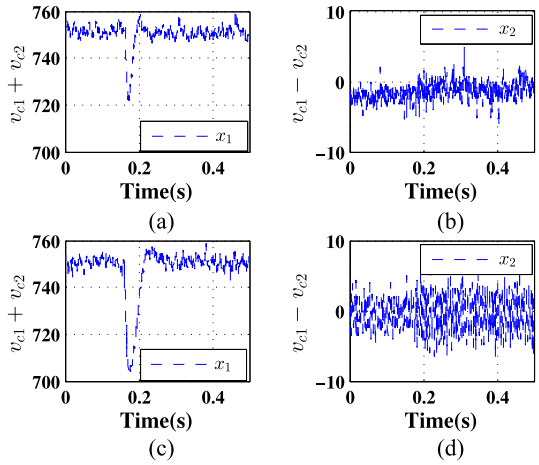

Fig. 9. Responses of the sum and difference of capacitor voltages x_1 and x_2. (a) and (b) Proposed control. (c) and (d) PI control.

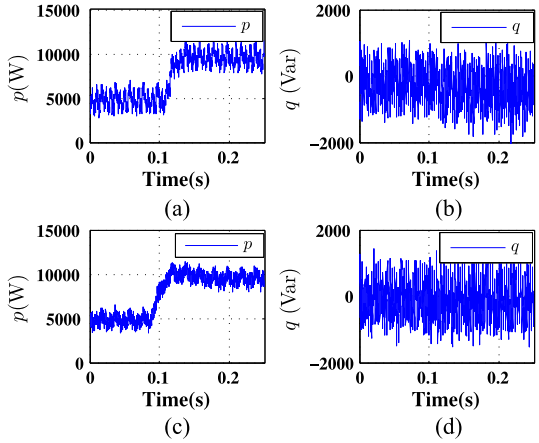

Fig. 10. Responses of active and reactive power p and q. (a) and (b) Proposed control. (c) and (d) PI control.

dynamics of v_{c1} and v_{c2} of our proposed and PI control strategy measured by oscilloscope, respectively. In the Fig. 9(a) and (c), one can observe that both control strategies are capable of regulating the dc-link output voltage x_1 to its desired value 750 V despite the load variation. However, it should be pointed out that the proposed control scheme has better performance, for example, it has faster dynamic response and less output voltage drop, especially during the transient process. Fig. 9(b) and (d) show the responses of the difference of capacitor voltages, in which we can see that, compared with the PI control, the voltage of the proposed strategy is smaller, almost close to zero.

The responses of active and reactive power are shown in the Fig. 10, respectively. It can be observed that both control strategies can enforce instantaneous active and reactive power p, q to track their references, respectively. The reference of instantaneous active power comes from the voltage regulation loop, which can regulate the output voltage, and the reference of instantaneous reactive power is 0 VAr to achieve unity power factor. Note that both control strategies can ensure that the active power steps from 4.6875 to 9.375 kW when load changes; in the meantime, the reactive power always remains 0 VAr. This demonstrates that both control strategies are robust to the

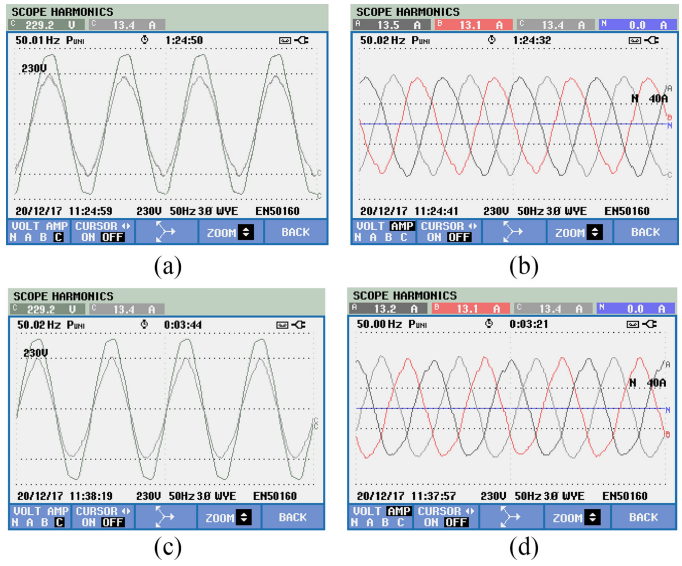

Fig. 11. Responses of grid voltage e_c and input current i_c and the three phase current. (a) and (b) Proposed control. (c) and (d) PI control.

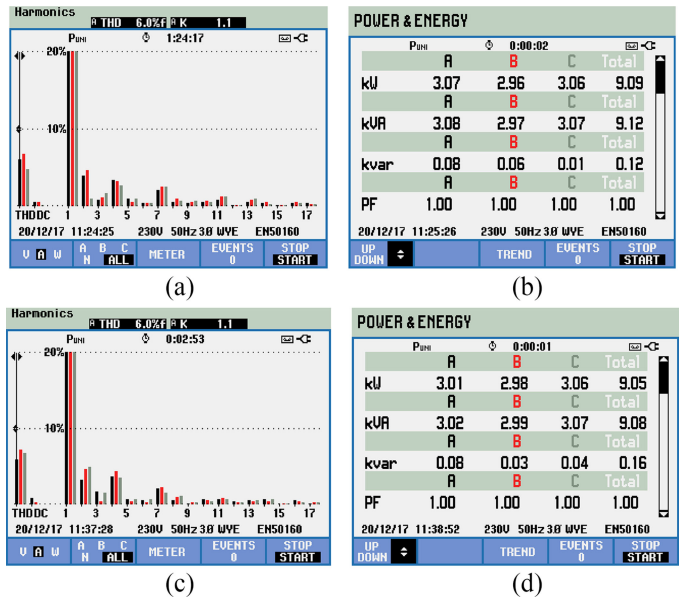

Fig. 12. Current harmonic spectrum, active and reactive power and power factor. (a) and (b) Proposed control. (c) and (d) PI control.

change of load. On the other hand, since reactive power has been kept close to 0 VAr, the grid source voltage has the same phase with the corresponding current (phase c voltage and current) as shown in Fig. 11(a) and (c), which means that the power factor is close to the unity as shown in Fig. 12(b) and (d). The dynamics of three phase current achieved with both control strategies are shown in the Fig. 11(b) and (d), and it can be seen from the Fig. 12(a) and (c) that the current total harmonic distortion (THD) of the both schemes has the same value. In fact, active and reactive power of both control strategies drawing from the grid is also almost the same, as can be seen in Fig. 12(b) and (d). Therefore, the experimental result demonstrates that the output voltage and difference of capacitor voltages of the proposed

control strategy have better performance than PI control with unity power factor.

V. Conclusion

In this paper, a novel control strategy has been proposed for three-phase three-level NPC power converter by taking advantage of cascade control structure including instantaneous power tracking control loop, voltage regulation loop, and voltage balancing loop. To deal with the model uncertainties of the system, a set of adaptive sliding mode controllers have been designed via RBF neural network technology in the instantaneous power tracking control loop. In the voltage regulation loop, an efficient but simple adaptive controller has been developed to regulate dc-link output voltage for simpler implementation. Then based on the reduced-order observer, an H_∞ controller combined with reduced-order observer is established to ensure imbalance voltages between two dc-link capacitors close to zero. Finally, the experimental results on the NPC converter have demonstrated that compared with the PI control, the output voltage of proposed control strategy has rather smaller voltage drop and remarkably shorter transient time and the difference of capacitor voltage of the proposed control strategy is smaller almost close to zero. Based on this fact, the devices of injecting a zero-sequence voltage and feedforward compensation can be replaced by our proposed control strategy, leading to the reduction of weight, size, and cost of the power converter. Furthermore, it can be observed that the proposed control strategy is robust to the change of load and has the significant value in practice. Our future work will focus on control to power converter under unbalanced grid-voltage conditions.

References

[1] T.-C. Ou, K.-H. Lu, and C.-J. Huang, "Improvement of transient stability in a hybrid power multi-system using a designed NIDC (novel intelligent damping controller)," *Energies*, vol. 10, no. 4, pp. 1–16, 2017.

[2] T.-C. Ou, "Ground fault current analysis with a direct building algorithm for microgrid distribution," *Int. J. Elect. Power Energy Syst.*, vol. 53, pp. 867–875, 2013.

[3] R. H. Lasseter and P. Paigi, "Microgrid: A conceptual solution," in *Proc. 35th Annu. Conf. IEEE Power Electron. Spec. Conf.*, vol. 6., 2004, pp. 4285–4290.

[4] T.-C. Ou, "A novel unsymmetrical faults analysis for microgrid distribution systems," *Int. J. Elect. Power Energy Syst.*, vol. 43, no. 1, pp. 1017–1024, 2012.

[5] E. Foruzan, L.-K. Soh, and S. Asgarpoor, "Reinforcement learning approach for optimal distributed energy management in a microgrid," *IEEE Trans. Power Syst.*, to be published, doi: 10.1109/TPWRS.2018.2823641.

[6] T.-C. Ou and C.-M. Hong, "Dynamic operation and control of microgrid hybrid power systems," *Energy*, vol. 66, pp. 314–323, 2014.

[7] Y. Deng, J. Li, K. H. Shin, T. Viitanen, M. Saeedifard, and R. G. Harley, "Improved modulation scheme for loss balancing of three-level active NPC converters," *IEEE Trans. Power Electron.*, vol. 32, no. 4, pp. 2521–2532, Apr. 2017.

[8] Q. Tabart, I. Vechiu, A. Etxeberria, and S. Bacha, "Hybrid energy storage system microgrids integration for power quality improvement using four-leg three-level NPC inverter and second-order sliding mode control," *IEEE Trans. Ind. Electron.*, vol. 65, no. 1, pp. 424–435, Jan. 2018.

[9] J. I. Leon, S. Vazquez, and L. G. Franquelo, "Multilevel converters: Control and modulation techniques for their operation and industrial applications," *Proc. IEEE*, vol. 105, no. 11, pp. 2066–2081, Nov. 2017.

[10] J. Rodriguez *et al.*, "Multilevel converters: An enabling technology for high-power applications," *Proc. IEEE*, vol. 97, no. 11, pp. 1786–1817, Nov. 2009.

[11] M. Malinowski, K. Gopakumar, J. Rodriguez, and M. A. Perez, "A survey on cascaded multilevel inverters," *IEEE Trans. Ind. Electron.*, vol. 57, no. 7, pp. 2197–2206, Jul. 2010.

[12] B. Zhao, Q. Song, J. Li, X. Xu, and W. Liu, "Comparative analysis of multilevel-high-frequency-link and multilevel-DC-link DC–DC transformers based on MMC and dual-active bridge for MVDC application," *IEEE Trans. Power Electron.*, vol. 33, no. 3, pp. 2035–2049, Mar. 2018.

[13] Z. Zhang, Z. Li, M. P. K. GAE, J. Rodriguez, and R. K. GAE, "Robust predictive control of three-level NPC back-to-back converter PMSG wind turbine systems with revised predictions," *IEEE Trans. Power Electron.*, to be published, doi: 10.1109/TPEL.2018.2796093.

[14] S. Vazquez, A. Marquez, R. Aguilera, D. Quevedo, J. I. Leon, and L. G. Franquelo, "Predictive optimal switching sequence direct power control for grid-connected power converters," *IEEE Trans. Ind. Electron.*, vol. 62, no. 4, pp. 2010–2020, Apr. 2015.

[15] P. Cortés, G. Ortiz, J. I. Yuz, J. Rodríguez, S. Vazquez, and L. G. Franquelo, "Model predictive control of an inverter with output LC filter for UPS applications," *IEEE Trans. Ind. Electron.*, vol. 56, no. 6, pp. 1875–1883, Jun. 2009.

[16] W. Mcmurray, "Fast response stepped-wave switching power converter circuit," U.S. Patent 3581212, May 25, 1971. [Online]. Available: https://www.google.com/patents/US3581212

[17] S. Alepuz, S. Busquets-Monge, J. Bordonau, J. Gago, D. González, and J. Balcells, "Interfacing renewable energy sources to the utility grid using a three-level inverter," *IEEE Trans. Ind. Electron.*, vol. 53, no. 5, pp. 1504–1511, Oct. 2006.

[18] E. Pouresmaeil, D. Montesinos-Miracle, and O. Gomis-Bellmunt, "Control scheme of three-level NPC inverter for integration of renewable energy resources into AC grid," *IEEE Syst. J.*, vol. 6, no. 2, pp. 242–253, Jun. 2012.

[19] H. R. Teymour, D. Sutanto, K. M. Muttaqi, and P. Ciufo, "Solar PV and battery storage integration using a new configuration of a three-level NPC inverter with advanced control strategy," *IEEE Trans. Energy Convers.*, vol. 29, no. 2, pp. 354–365, Jun. 2014.

[20] H.-J. Kim, H.-D. Lee, and S.-K. Sul, "A new PWM strategy for common-mode voltage reduction in neutral-point-clamped inverter-fed AC motor drives," *IEEE Trans. Ind. Appl.*, vol. 37, no. 6, pp. 1840–1845, Nov.-Dec. 2001.

[21] K. Matsui, Y. Kawata, and F. Ueda, "Application of parallel connected NPC-PWM inverters with multilevel modulation for AC motor drive," *IEEE Trans. Power Electron.*, vol. 15, no. 5, pp. 901–907, Sep. 2000.

[22] H. B. Abdelghani, A. B. Benabdelghani, I. Slama-Belkhodja, and D. Montesinos-Miracle, "Fault tolerant NPC converter control for isolated PV sytems: Application for an isolated telecommunication center," in *Proc 16th IEEE Mediterranean Electrotechnical Conf.*, 2012, pp. 319–324.

[23] S. Kouro, J. Rodriguez, B. Wu, S. Bernet, and M. Perez, "Powering the future of industry: High-power adjustable speed drive topologies," *IEEE Ind. Appl. Mag.*, vol. 18, no. 4, pp. 26–39, Jul.–Aug. 2012.

[24] R. Katebi, J. He, and N. Weise, "Advanced three-level active neutral-point clamped converter with improved fault-tolerant capabilities," *IEEE Trans. Power Electron.*, vol. 33, no. 8, pp. 6897–6909, Aug. 2018.

[25] J. I. Leon, S. Kouro, L. G. Franquelo, J. Rodriguez, and B. Wu, "The essential role and the continuous evolution of modulation techniques for voltage-source inverters in the past, present, and future power electronics," *IEEE Trans. Ind. Electron.*, vol. 63, no. 5, pp. 2688–2701, May 2016.

[26] V. Blasko and V. Kaura, "A new mathematical model and control of a three-phase AC-DC voltage source converter," *IEEE Trans. Power Electron.*, vol. 12, no. 1, pp. 116–123, Jan. 1997.

[27] J. D. Barros and J. F. Silva, "Optimal predictive control of three-phase NPC multilevel converter for power quality applications," *IEEE Trans. Ind. Electron.*, vol. 55, no. 10, pp. 3670–3681, Oct. 2008.

[28] V. Yaramasu and B. Wu, "Predictive control of a three-level boost converter and an NPC inverter for high-power PMSG-based medium voltage wind energy conversion systems," *IEEE Trans. Power Electron.*, vol. 29, no. 10, pp. 5308–5322, Oct. 2014.

[29] S. Vazquez *et al.*, "Model predictive control for single-phase NPC converters based on optimal switching sequences," *IEEE Trans. Ind. Electron.*, vol. 63, no. 12, pp. 7533–7541, Dec. 2016.

[30] F. Sebaaly, H. Vahedi, H. Y. Kanaan, N. Moubayed, and K. Al-Haddad, "Design and implementation of space vector modulation-based sliding mode control for grid-connected 3L-NPC inverter," *IEEE Trans. Ind. Electron.*, vol. 63, no. 12, pp. 7854–7863, Dec. 2016.

[31] F. Sebaaly, H. Vahedi, H. Kanaan, N. Moubayed, and K. Al-Haddad, "Sliding-mode current control design for a grid-connected three-level NPC inverter," in *Proc Int. Conf. Renewable Energies for Developing Countries*, 2014, pp. 217–222.
[32] M. Seixas, R. Melício, and V. M. F. Mendes, "Offshore wind turbine simulation: Multibody drive train. Back-to-back NPC (neutral point clamped) converters. Fractional-order control," *Energy*, vol. 69, pp. 357–369, 2014.
[33] R. Portillo, S. Vazquez, J. I. Leon, M. M. Prats, and L. G. Franquelo, "Model based adaptive direct power control for three-level npc converters," *IEEE Trans. Ind. Informa.*, vol. 9, no. 2, pp. 1148–1157, May 2013.
[34] S. Vazquez, J. Liu, H. Gao, and L. G. Franquelo, "Second order sliding mode control for three-level NPC converters via extended state observer," in *Proc. 41st Annu. Conf. IEEE Ind. Electron. Soc.,* 2015, pp. 005 118–005 123.
[35] F. Umbría, F. Gordillo, F. Gomez-Estern, F. Salas, R. C. Portillo, and S. Vázquez, "Voltage balancing in three-level neutral-point-clamped converters via Luenberger observer," *Control Eng. Pract.*, vol. 25, pp. 36–44, Apr. 2014.
[36] H. Akagi E. H. Watanabe, and M. Aredes, *Instantaneous power theory and applications to power conditioning*. New Jersey, NJ, USA: Wiley, 2017.
[37] X. Liu and J. Cao, "Robust state estimation for neural networks with discontinuous activations," *IEEE Trans. Syst. Man Cybern. B (Cybern)*, vol. 40, no. 6, pp. 1425–1437, Dec. 2010.
[38] N. Liu and J. Fei, "Adaptive fractional sliding mode control of active power filter based on dual RBF neural networks," *IEEE Access*, vol. 5, pp. 27 590–27 598, 2017.
[39] D. Shevitz and B. Paden, "Lyapunov stability theory of nonsmooth systems," *IEEE Trans. Autom. Control*, vol. 39, no. 9, pp. 1910–1914, Sep. 1994.
[40] P. Gahinet, A. Nemirovskii, A. J. Laub, and M. Chilali, "The LMI control toolbox," in *Proc. 33rd Conf. IEEE Decisi. Control,* vol. 3., 1994, pp. 2038–2041.
[41] J. C. Doyle, K. Glover, P. P. Khargonekar, and B. A. Francis, "State-space solutions to standard H_2 and H_∞ control problems," *IEEE Trans. Autom. Control*, vol. 34, no. 8, pp. 831–847, Aug. 1989.

Yunfei Yin received the B.S. degree in electrical engineering and automation from China Petroleum University, Dongying, China, in 2013, the M.E. degree in control theory and control engineering from Bohai University, Jinzhou, China, in 2016. He is currently working toward the Ph.D. degree at the Harbin Institute of Technology, Harbin, China.

His current research interests include switched control, sliding mode control, adaptive control and their applications to power electronic systems for renewable energy systems.

Jianxing Liu (M'13) received the B.S. degree in mechanical engineering in 2008, the M.E. degree in control science and engineering in 2010, both from the Harbin Institute of Technology, Harbin, China, and the Ph.D. degree in automation from the Technical University of Belfort-Montbeliard, Belfort, France, in 2014.

Since 2014, he joined Harbin Institute of Technology as a faulty member. His current research interests include nonlinear control algorithms, sliding mode control, fuel cell systems, hybrid electric or fuel cell vehicles, control of power electronics and converters, wind-driven generator systems, energy management for micro-grids, nonlinear control and observation methods, and their applications in industrial electronics systems and renewable energy systems.

Juan Antonio Sánchez was born in Moron, Seville, Spain, in 1974. He received the B.S., M.S., and Ph.D. degrees in industrial engineering, all from the University of Seville, Seville, in 2001, 2004, and 2017, respectively.

He is currently an Associate Professor with the Department of Electronic Engineering, University of Seville. His research interests include power active filters, power converters control, and industrial drives.

Sergio Vazquez (S'04–M'08–SM'14) was born in Seville, Spain, in 1974. He received the M.S. and Ph.D. degrees in industrial engineering from the University of Seville, Seville, in 2006 and 2010, respectively.

Since 2002, he is with the Power Electronics Group working in R&D projects. He is an Associate Professor with the Department of Electronic Engineering, University of Seville. His research interests include power electronics systems, modeling, modulation and control of power electronics converters applied to renewable energy technologies.

Dr. Vazquez was the recipient as coauthor of the 2012 Best Paper Award of the IEEE TRANSACTIONS ON INDUSTRIAL ELECTRONICS and 2015 Best Paper Award of the IEEE INDUSTRIAL ELECTRONICS MAGAZINE. He is involved in the Energy Storage Technical Committee of the IEEE Industrial Electronics Society and is currently serving as an Associate Editor of the IEEE TRANSACTIONS ON INDUSTRIAL ELECTRONICS.

Ligang Wu (M'10–SM'12) received the B.S. degree in automation from the Harbin University of Science and Technology, Harbin, China, in 2001, and the M.E. degree in navigation guidance and control and the Ph.D. degree in control theory and control engineering in 2003 and 2006, respectively, both from the Harbin Institute of Technology, Harbin, China.

From January 2006 to April 2007, he was a Research Associate with the Department of Mechanical Engineering, The University of Hong Kong, Hong Kong. From September 2007 to June 2008, he was a Senior Research Associate with the Department of Mathematics, City University of Hong Kong, Hong Kong. From December 2012 to December 2013, he was a Research Associate with the Department of Electrical and Electronic Engineering, Imperial College London, London, U.K. In 2008, he joined the Harbin Institute of Technology as an Associate Professor and was then promoted to a Full Professor in 2012. He has authored or coauthored 6 research monographs and more than 150 research papers in international referred journals. His current research interests include switched systems, stochastic systems, computational and intelligent systems, multidimensional systems, sliding mode control, and flight control.

Dr. Wu was the winner of the National Science Fund for Distinguished Young Scholars in 2015, and received the China Young Five Four Medal in 2016. He was named as the Distinguished Professor of Yangtze River Scholar in 2017, and was named as the Highly Cited Researcher in 2015, 2016, and 2017. He is currently an Associate Editor for a number of journals, including IEEE TRANSACTIONS ON AUTOMATIC CONTROL, IEEE/ASME TRANSACTIONS ON MECHATRONICS, *Information Sciences, Signal Processing*, and *IET Control Theory and Applications*. He is also an Associate Editor for the Conference Editorial Board, IEEE Control Systems Society.

Jose I. Leon (F'17) was born in Cadiz, Spain. He received the B.S., M.S., and Ph.D. degrees in telecommunications engineering from the Universidad de Sevilla, Seville, Spain, in 1999, 2001, and 2006, respectively.

He is currently an Associate Professor with the Department of Electronic Engineering, Universidad de Sevilla. His research interests include modulation and control of power converters for high-power applications and renewable energy systems.

Dr. Leon was the corecipient of the 2008 Best Paper Award of IEEE INDUSTRIAL ELECTRONICS MAGAZINE, the 2012 Best Paper Award of the IEEE TRANSACTIONS ON INDUSTRIAL ELECTRONICS, and the 2015 Best Paper Award of IEEE INDUSTRIAL ELECTRONICS MAGAZINE. He was the recipient of the 2014 IEEE J. David Irwin Industrial Electronics Society Early Career Award and the 2017 IEEE Bimal K. Bose Energy Systems Award. He is currently serving as an Associate Editor of the IEEE TRANSACTIONS ON INDUSTRIAL ELECTRONICS.

Leopoldo G. Franquelo (M'84–SM'96–F'05) was born in Malaga, Spain. He received the M.Sc. and Ph.D. degrees in electrical engineering from the Universidad de Sevilla, Seville, Spain, in 1977 and 1980, respectively.

His current research interest lies on modulation techniques for multilevel inverters and its application to power electronic systems for renewable energy systems.

Dr. Franquelo has been an Industrial Electronics Society (IES) Distinguished Lecturer since 2006, an Associate Editor for the IEEE Transactions on Industrial Electronics since 2007, Co-Editor-in-Chief since 2014, and Editor-in-Chief since 2015. He was a Member-at-Large of the IES AdCom (2002–2003), the Vice President for Conferences (2004–2007), and the President Elect of the IES (2008–2009). He was the President of the IEEE Industrial Electronics Society (2010–2011) and currently is IES AdCom Life member. He has received a number of Best Paper Awards from journals of the IEEE. In 2012 and 2015, he received the Eugene Mittelmann Award and the Anthony J. Hornfeck Service Award from IES, respectively.